

Insertion of Isonitriles into the M–C Bonds of Group 4 Dialkyl Complexes

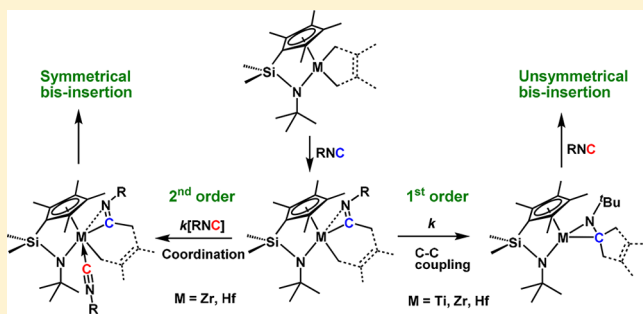
Jiawei Chen,[‡] Nadine Yassin,[†] Thilina Gunasekara,[‡] Jack R. Norton,^{*,‡} and Michael Rauch[‡]

[‡]Department of Chemistry, Columbia University, 3000 Broadway, New York, New York 10027, United States

[†]Department of Chemistry, Barnard College, 3009 Broadway, New York, New York 10027, United States

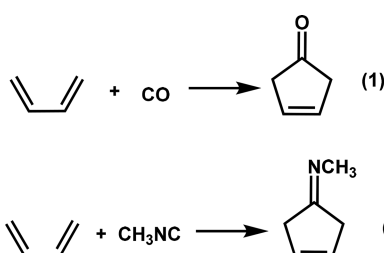
Supporting Information

ABSTRACT: The 2,3-dimethylbutadiene complexes of Group 4 metals with constrained geometry (cg) ligands have been prepared and found to adopt a supine orientation with σ^2, π bonding. Treatment of cgTi(2,3-dimethylbutadiene) (**1-Ti**) with $^t\text{BuNC}$ leads to the formation of a titana-aziridine (**3**) with a coordinated cyclopentenimine that arises from the formal [4+1] addition of the diene to the isonitrile. In contrast, the reactions of cgZr(2,3-dimethylbutadiene) (**1-Zr**) or cgHf(2,3-dimethylbutadiene) (**1-Hf**) with 2 equiv of $^t\text{BuNC}$ or XyNC proceeded in a more sophisticated manner to yield unsymmetrical 2,5-diazamettallacyclopentane derivatives (**4**, **6-Zr**, and **6-Hf**) or symmetrical 2,5-diazamettallacyclopentene complexes (**7-Zr** and **7-Hf**). The unsymmetrical products contain coordinated cyclopropanes; the strength of the interaction is measured by the reduction in the $^1\text{J}_{\text{CC}}$ of the C–C bond that is coordinated. A detailed mechanistic analysis has been possible with the related cgM(Me)₂ (M = Ti and Hf) complexes. The first insertion is too fast to monitor, but allows complete conversion to an alkyl iminoacyl intermediate. The second isonitrile (RNC) may react with that intermediate by either of two different mechanisms, reductive elimination and coordination/insertion. In the first mechanism (Ti), rate-determining C–C coupling gives a titana-aziridine, followed by fast coordination of the isonitrile. In the second mechanism (Hf), coordination is the slow step; insertion to form a bis(iminoacyl) Hf complex is rapid.



INTRODUCTION

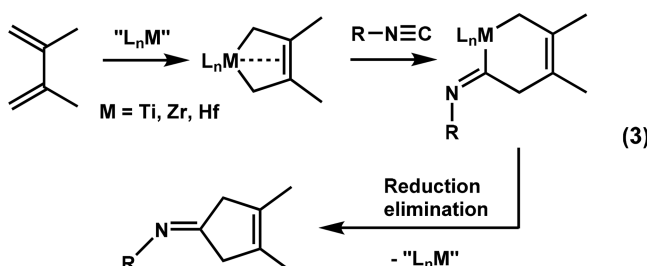
Reactions such as the [4+1] addition of SO_2 to dienes¹ and the [2+2+1] addition of CO to enynes² are familiar and useful approaches to the construction of five-membered rings. The stoichiometric [4+1] cycloaddition of CO to dienes was accomplished by Corey and co-workers in 1972,³ there have been reports of the carbonylation of iron diene complexes,⁴ and a diallene has been carbonylated catalytically.⁵ However, the catalytic synthesis of a cyclopentenone from CO and a diene (eq 1) remains a challenge.⁶



Isonitriles, isoelectronic with CO, are attractive replacements for it in cycloaddition reactions. Spartan calculations show that eq 2 is considerably more downhill thermodynamically than eq 1.⁷ Isonitriles are easier to handle in the laboratory than CO,

and their steric and electronic properties are readily tuned by variation of the substituent. Both the stoichiometric⁸ and the catalytic⁹ cycloadditions of RNC to α,β -unsaturated carbonyl compounds, as well as the Ni-promoted¹⁰ and Ti-catalyzed¹¹ [2+2+1] cyclizations of RNC to enynes, are known.

The obvious diene complexes to examine in this connection are those of Group 4 elements. Their bonding is best described by σ^2, π resonance structures,¹² which should permit facile insertions of RNC and perhaps catalyze eq 2 by the sequence in eq 3.

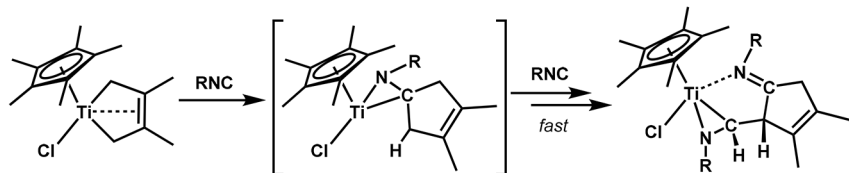
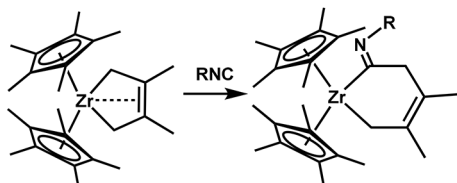
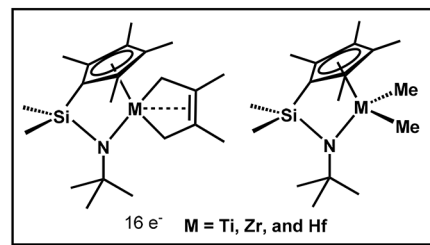


Two classes of Group 4 diene complexes, $\text{Cp}^*(\text{Cl})\text{M}(\text{diene})$ ($\text{M} = \text{Ti}$ and Hf) and $\text{Cp}^*_{\text{Zr}}(\text{diene})$, are well known, and the

Received: May 22, 2018

Published: June 15, 2018

Scheme 1. Known RNC Insertion Chemistry of Group 4 Diene Complexes and cg Complexes To Be Studied

a) $14 e^-$, multiple insertions with H shift:b) $18 e^-$, one insertion without further C-C coupling:*This work:*

reactions of both with isonitriles have been examined.¹³ The RNC reactions of $Cp^*(Cl)M(\text{diene})$ are complex,¹⁴ probably because their coordinative unsaturation encourages multiple insertions; the $Cp^*_2Zr(\text{diene})$ complexes are not only difficult to prepare but relatively slow to react with isonitriles, probably because their coordinative saturation discourages insertion.

Although the insertion of isonitriles into M–C bonds has been used as a tool for construction of new C–C bonds,^{15–17} there has been little mechanistic study of such insertions. Their rates have often been too fast for convenient study. In one case ($M-\text{CH}_3$ with a calix[4]arene ligand^{16m,18}) calculations have implied that the rate-determining step is the coordination of the RNC.

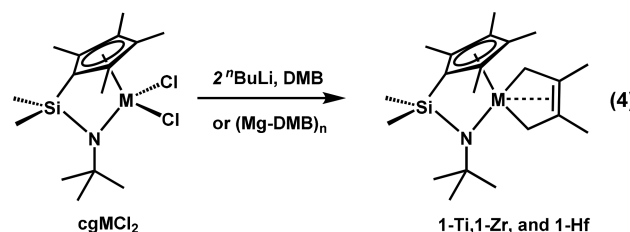
We have therefore examined the preparation and insertion reactions of the diene and dimethyl complexes of the constrained geometry (cg) ligand ($\eta^5\text{-C}_5\text{Me}_4\text{Me}_2\text{Si}(\eta^1\text{-N}^t\text{Bu})$)¹⁹ (Scheme 1). Constrained geometry complexes of Group 4 metals²⁰ have been widely studied as catalysts for olefin polymerization^{20b,21}—although the reasons for their catalytic activity are not entirely clear.²² They are not only promising catalysts for [4+1] cycloadditions but are ideal for the study of the mechanisms of RNC insertion.

Several cgTi diene complexes, including that of 2,3-dimethylbutadiene (DMB), were reported by Devore, Marks, and co-workers in 1995.²³ A series of cgTi and cgZr diene complexes were prepared by Erker and co-workers from magnesium dienes in 2000,²⁴ while Petersen and co-workers synthesized additional cgTi and cgZr diene complexes.²⁵ We have examined the RNC chemistry of the DMB complexes of cgTi, cgZr, and cgHf, and of the dimethyl complexes of cgTi and cgHf.^{16,26} We have studied the kinetics and mechanism of RNC insertion into the M–C bonds of cgTi(Me)₂ and cgHf(Me)₂.

RESULTS AND DISCUSSION

1. CgM(DMB) Complexes and Their Reactions with Isonitriles. *1.1. Synthesis of cgM(2,3-dimethylbutadiene) Complexes (M = Ti, Zr and Hf).* As Devore and Marks had reported, the reaction of cgTiCl₂ with 2 equiv of ⁷BuLi in the presence of excess DMB gave the deeply colored solid cgTi(DMB) (1-Ti, eq 4). Recrystallization from pentane at -30°C gave pure 1-Ti in a yield of 45%.

The analogous Zr and Hf compounds were prepared by a method like that reported by Erker for other diene complexes of Zr: treatment of the dichlorides cgZrCl₂ and cgHfCl₂ with the magnesium-diene reagent (Mg-DMB)_n. Red crystalline cgZr(DMB) (1-Zr, eq 4) and yellow crystalline cgHf(DMB) (1-Hf, eq 4) were obtained in yields of 65% and 67%, respectively.



Structure of, and Bonding in, the Ti DMB Complex 1-Ti. A single-crystal X-ray diffraction (SC-XRD) structure (Figure 1) shows a “supine” orientation for the DMB in 1-Ti.²⁷ The internal C–C bond is 0.087 Å shorter than the terminal C–C bonds (see Table 1), showing that the DMB is best described as a metallacycle; this conclusion is supported by the large difference between the Ti–C_{internal} and the Ti–C_{terminal} distances (also in Table 1), around 0.301 Å.²⁸ As expected from earlier observations by Erker and by Nakamura the internal double bond of the metallacycle is weakly coordinated, giving 1-Ti σ^2, π character. (All of the possible combinations of “supine/prone” and σ^2, π / π^2 are drawn above Table 1.)

Devore and co-workers reported^{23b} two ¹H NMR signals for the protons (H_{anti} and H_{syn}) on the terminal carbons of cgTi(DMB) (1-Ti): a broad one at δ 1.70 and a broad doublet at δ 2.06. At room temperature we observe the second (δ 2.06) signal but not the first; we do see another averaged peak, a broad signal at δ 1.25 which sharpens at $+60^\circ\text{C}$ —surely the other set of H’s on the terminal carbons. We do find (¹H-coupled ¹³C NMR) identical $^1J_{\text{CH}}$ values, 142 Hz, for both of these H’s—a value in between the ones expected for the metallacycle (σ^2, π) and diene (π^2) descriptions.

Structure of, and Bonding in, the Zr and Hf DMB Complexes 1-Zr and 1-Hf. We obtained X-ray-quality crystals for cgZr(DMB) (1-Zr) and cgHf(DMB) (1-Hf) by recrystallization from cold hexanes. The resulting SC-XRD structures show that,

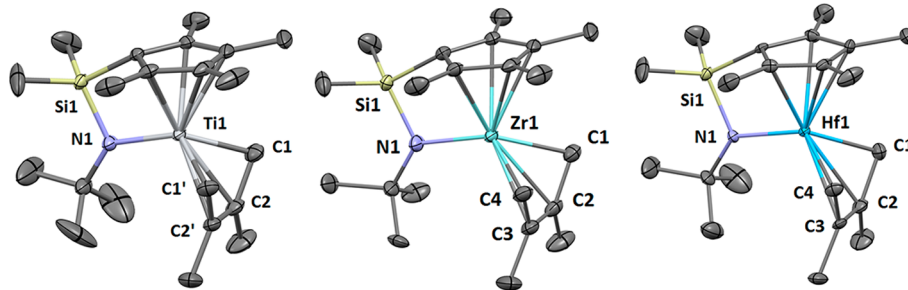
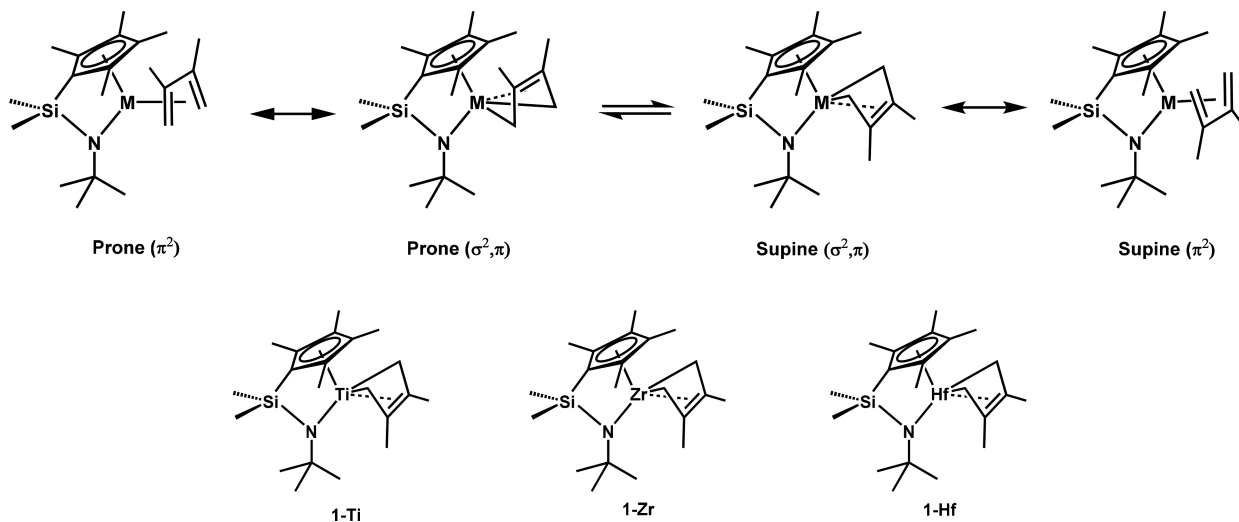


Figure 1. Structures of cgTi(DMB) (**1-Ti**), cgZr(DMB) (**1-Zr**), and cgHf(DMB) (**1-Hf**). Selected interatomic distances (Å) and angles (deg): a) Ti1–N1 2.022(2), Ti1–C1 2.149(2), Ti1–C2 2.450(2), C1–C2 1.454(3), C2–C2' 1.367(5); b) Zr1–N1 2.138(3), Zr1–C1 2.263(3), Zr1–C2 2.523(3), Zr1–C3 2.541(3), Zr1–C4 2.290(3), C1–C2 1.459(4), C2–C3 1.384(4), C3–C4 1.463(4); c) Hf1–N1 2.121(5), Hf1–C1 2.221(5), Hf1–C2 2.539(5), Hf1–C3 2.557(5), Hf1–C4 2.252(5), C1–C2 1.480(7), C2–C3 1.374(7), C3–C4 1.475(7).

Table 1. Comparison of Structural Features of cgM(DMB) **1-Ti, **1-Zr**, and **1-Hf****

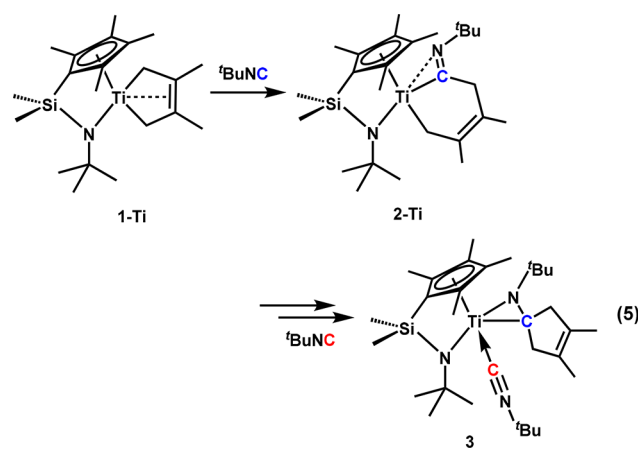


compd	M	δ (ppm)							
		H _{syn}	H _{anti}	$^2J_{HH}$ (Hz)	$^1J_{CH}$ (Hz)	M–N (Å)	ΔMC^a (Å)	ΔCC^a (Å)	orientation
1-Ti	Ti	2.06 (d)	1.25 (br)	8.5	142	2.022(2)	0.301	0.087	supine
1-Zr	Zr	2.54 (d)	−0.48 (d)	10	129; 149	2.138(2)	0.256	0.077	supine
1-Hf	Hf	1.86 (br)	0.06 (br)	nr	134; 138	2.121(5)	0.312	0.104	supine

^a $\Delta MC = d(M-C_{\text{terminal}}) - d(M-C_{\text{internal}})$; $\Delta CC = [d(C1-C2) + d(C3-C4)]/2 - d(C2-C3)$. As **1-Ti** has a mirror plane, $d(C1-C2) = d(C3-C4)$. nr = not resolved.

like the Ti complex, the Zr and Hf complexes adopt a supine orientation for their diene ligands. The difference between the metal–terminal carbon distance and the metal–internal carbon distance (ΔMC in Table 1) is 0.256 and 0.312 Å for **1-Zr** and **1-Hf**, respectively, indicating that in the solid state both **1-Zr** and **1-Hf** adopt metallacycle (σ^2, π) resonance structures; the positive values of ΔCC confirm this conclusion.²⁹ The solution ¹H NMR is again not structurally definitive. For the Zr-diene complex **1-Zr**, the H's on the terminal carbon (H_{anti} and H_{syn}) appear as doublets at δ 2.54 and δ −0.48, with $^1J_{CH}$ values of 129 and 149 Hz. For the Hf-diene complex **1-Hf**, the H_{anti} and H_{syn} signals are two broad features at δ 1.86 and δ 0.06, with $^1J_{CH}$ = 134 and 138 Hz, respectively.

1.2. Isonitriles Insertion into cgM(DMB) Complexes. Insertion of Isonitriles into cgTi(DMB) **1-Ti.** The reaction of **1-Ti** with >2 equiv of *tert*-butyl isonitrile ^tBuNC (eq 5) led to rapid formation of a species with two isonitrile ^tBu signals in the ¹H NMR, along with two AB spin systems with the same $^2J_{HH}$ of 17 Hz. ¹³C NMR confirmed two methylene carbons, δ 49.8 and 56.6, with



the same $^1J_{CH}$ of 125 Hz for all H's. ¹³C also showed the absence of an iminoacyl carbon, the presence of a coordinated ^tBuNC (at δ 173.2), and a η^2 -coordinated imine carbon (at δ 74.6). We speculated that the product might be a titana-aziridine with an

additional coordinated $^t\text{BuNC}$ (**3**)—generated by reductive elimination of an iminoacyl intermediate (**2**–Ti from the first insertion) and coordination of a second $^t\text{BuNC}$. An SC-XRD structure (**Figure 2**) confirmed this proposal. A cyclopentenimine

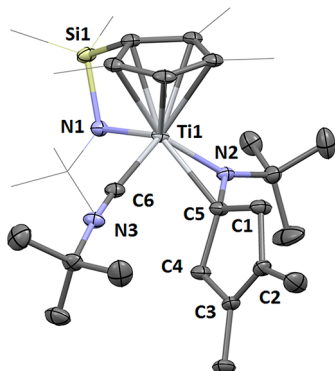


Figure 2. SC-XRD structure of **3**. Selected interatomic distances (\AA) and angles (deg): Ti1–N1 2.000(1), Ti1–N2 1.908(1), Ti1–C5 2.212(2), Ti1–C6 2.142(2), N2–C5 1.393(2), N3–C6 1.154(2).

(formally the result of a [4+1] addition) is coordinated in η^2 fashion to the Ti, with the nitrogen away from the coordinated $^t\text{BuNC}$. The C–N distance within the imine, 1.393(2) \AA , is consistent with the single bond implied by the titana-aziridine description. For the coordinated $^t\text{BuNC}$, the short C–N distance of 1.154(2) \AA and the small deviation of the C–N–C from a linear geometry (angle 173.5°) are consistent with the minimal backbonding that is expected.^{16g,o,17a,30}

In the absence of added $^t\text{BuNC}$ a C_6D_6 solution of **3** decomposes to a complex mixture of intractable species. In the presence of excess $^t\text{BuNC}$ **3** does not undergo further insertion and the cyclopentenimine is not lost.

Insertion of Isonitriles into $\text{cgHf}(\text{DMB})\text{1-Hf}$ and $\text{cgZr}(\text{DMB})\text{1-Zr}$. When 1 equiv of $^t\text{BuNC}$ was added to the Hf-diene **1-Hf** compound, the monoinsertion product **2-Hf** formed rapidly and cleanly (**eq 6**). SC-XRD analysis (**Figure 3**) revealed the

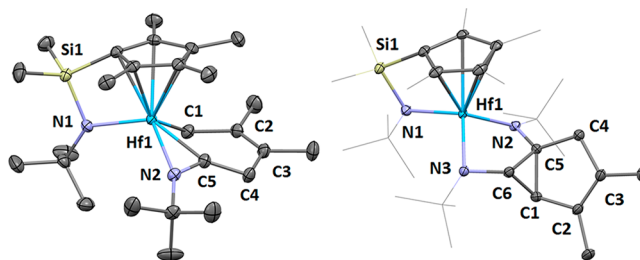
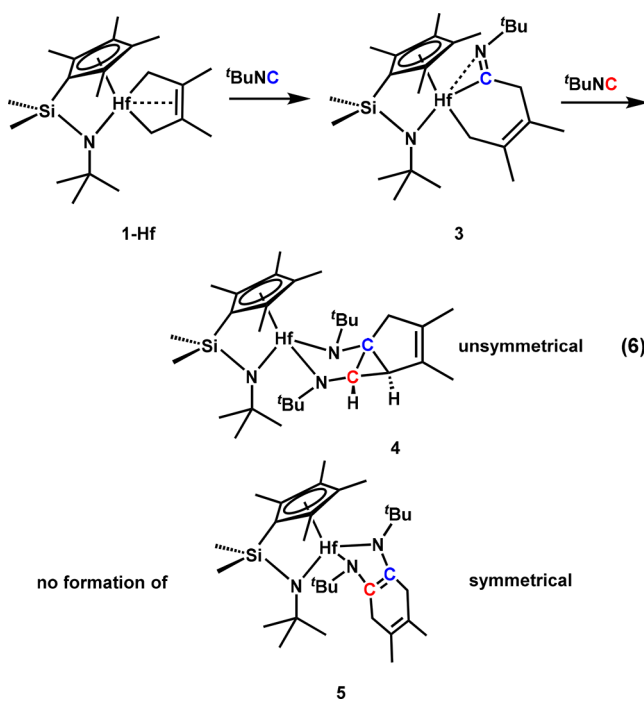


Figure 3. Structures of compound **2-Hf** and **4**. Selected interatomic distances (\AA) and angles (deg): a) Hf1–N1 2.107(2), Hf1–N2 2.224(2), Hf1–C1 2.294(2), Hf1–C5 2.138(2), N2–C5 1.277(2); b) Hf1–N1 2.109(1), Hf1–N2 2.061(1), Hf1–N3 2.038(1), Hf1–C5 2.608(2), Hf1–C6 2.568(2), N2–C5 1.443(2), N3–C6 1.435(2), C1–C5 1.528(2), C1–C6 1.527(2), C5–C6 1.585(2).

formation of a cyclic iminoacyl species that is consistent with the isonitrile insertion into one of the Hf–C bonds of the metallacyclopentene precursor. The η^2 coordination with “N-outside”³¹ of the iminoacyl to the Hf is reflected in the short Hf1–N2 distance of 2.224(2) \AA .

Addition of another equivalent of $^t\text{BuNC}$ to **2-Hf** (eq 6) to exclusive formation of the *unsymmetrical* bis-insertion product **4**, obviously the result of a hydride shift at some point. We did not observe the formation of any of the symmetrical bis-insertion product **5**. The X-ray structure of **4** (**Figure 3**) clearly shows a cyclopropane ring. One edge of that ring features short Hf–C contacts of 2.608(2) and 2.568(2) \AA , indicating formation of a σ complex between the C5–C6 bond and the metal.³² That interaction results in the elongation of that C–C bond to 1.585(2) \AA , considerably longer than the other C–C bonds (1.528(2) and 1.527(2) \AA) in the cyclopropane ring.

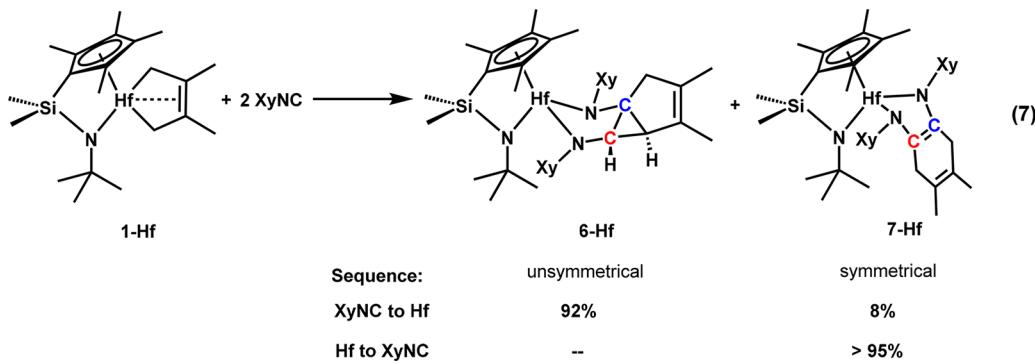
With 2,6-dimethylphenyl isonitrile (xylyl isonitrile, XyNC) the same reaction (with **1-Hf**, eq 7) led to a mixture of bis-insertion products, one (**6-Hf**) like **4** and the other (**7-Hf**) like **5**. The ratio, as expected, depended (see **Scheme 2**) on the concentration of XyNC. For example, with slow addition of 2 equiv of XyNC to a solution of **1-Hf**, we obtained **6-Hf** as the major product (92%), accompanied by **7-Hf** as the minor product (8%). If the addition sequence was reversed, the formation of the symmetrical isomer **7-Hf** was almost quantitative (>95%).

We then examined the analogous reactions between **1-Zr** and isonitriles. The reaction between **1-Zr** and $^t\text{BuNC}$ gave an intractable mixture. However, reactions between **1-Zr** and XyNC resulted in mixtures of the unsymmetrical product **6-Zr** and the symmetrical product **7-Zr** (eq 8). Again, the product distribution could be adjusted (see **Scheme 3**) by changing the ratio of the reactants. Both **6-Zr** and **7-Zr** were isolated.

We were able to obtain X-ray structures (**Figure 4**) for **7-Zr** and **7-Hf**. Both adopt a supine orientation for the folded diazametallacycle, similar to that of the $\text{cgM}(\text{diene})$ compounds. The new ligand features an enediamido rather than a diazabutadiene resonance form for both Zr and Hf, as indicated by the long–short–long alternation of bond lengths in the N–C=C–N moiety.^{16k,33} The enediamido C=C coordinates to the metal in both **7-Zr** ($\text{Zr1}\cdots\text{C5}$ 2.582(4) \AA , $\text{Zr1}\cdots\text{C6}$ 2.573(4) \AA) and **7-Hf** ($\text{Hf1}\cdots\text{C5}$ 2.591(3) \AA , $\text{Hf1}\cdots\text{C6}$ 2.589(3) \AA). The coordinated C=C is slightly longer than the uncoordinated one (1.382(5) vs 1.329(6) \AA for Zr; and 1.370(5) vs 1.335(6) \AA for Hf).

$^1\text{J}_{\text{CC}}$ in Coordinated Cyclopropanes. The coordination of cyclopropanes to Group 4 elements is sufficiently rare that it is worth measuring the strength of that interaction in **4** and **6**.

Scheme 2. Reaction between 1-Hf and XyNC under Different Conditions



Scheme 3. Reaction between 1-Zr and XyNC under Different Conditions

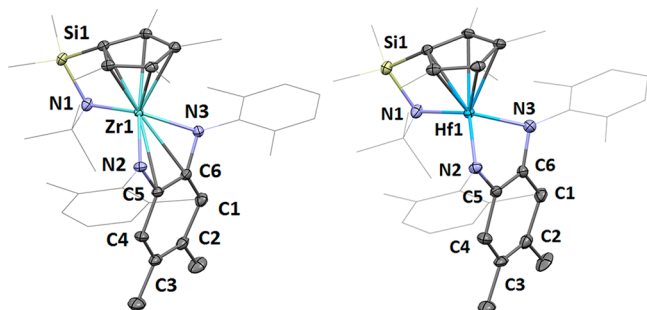
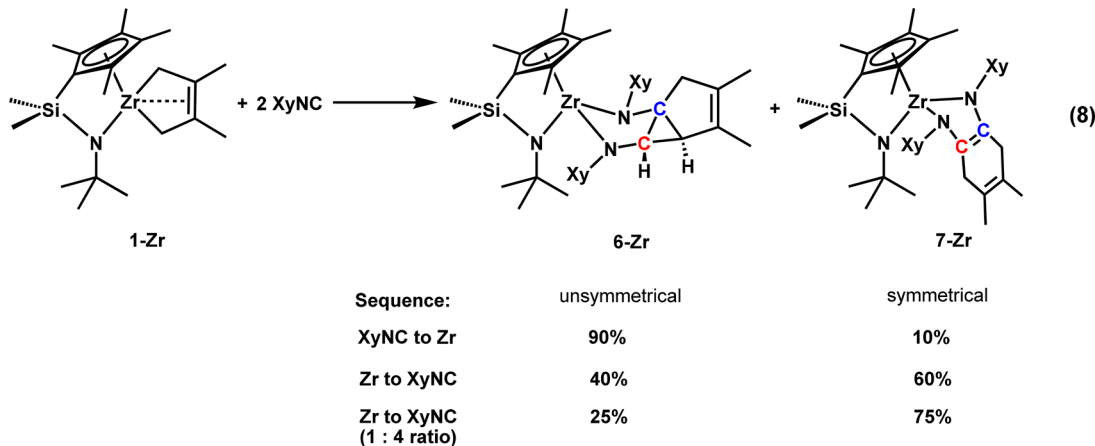
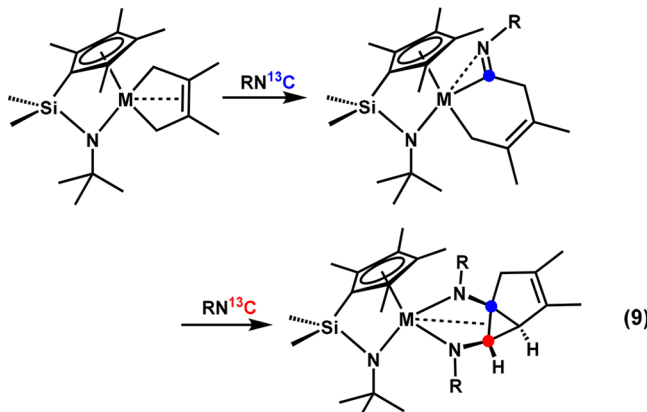


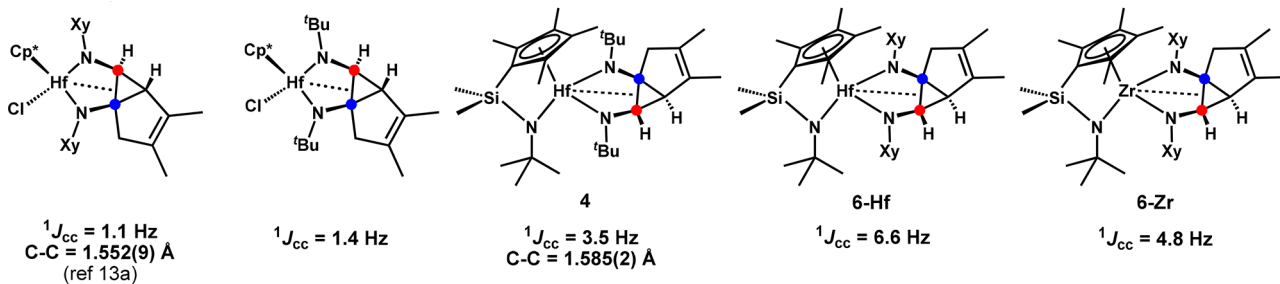
Figure 4. X-ray structures of symmetrical bis-insertion complexes of 7-Zr and 7-Hf. Selected interatomic distances (Å) and angles (deg): a) Zr1–N1 2.153(3), Zr1–N2 2.094(3), Zr1–N3 2.076(3), Zr1–C5 2.582(4), Zr1–C6 2.573(4), N2–C5 1.407(5), N3–C6 1.417(5), C5–C6 1.382(5), C2–C3 1.329(6); b) Hf1–N1 2.130(3), Hf1–N2 2.075(3), Hf1–N3 2.057(3), Hf1–C5 2.591(3), Hf1–C6 2.589(3), N2–C5 1.416(5), N3–C6 1.426(4), C5–C6 1.370(5), C2–C3 1.335(6).



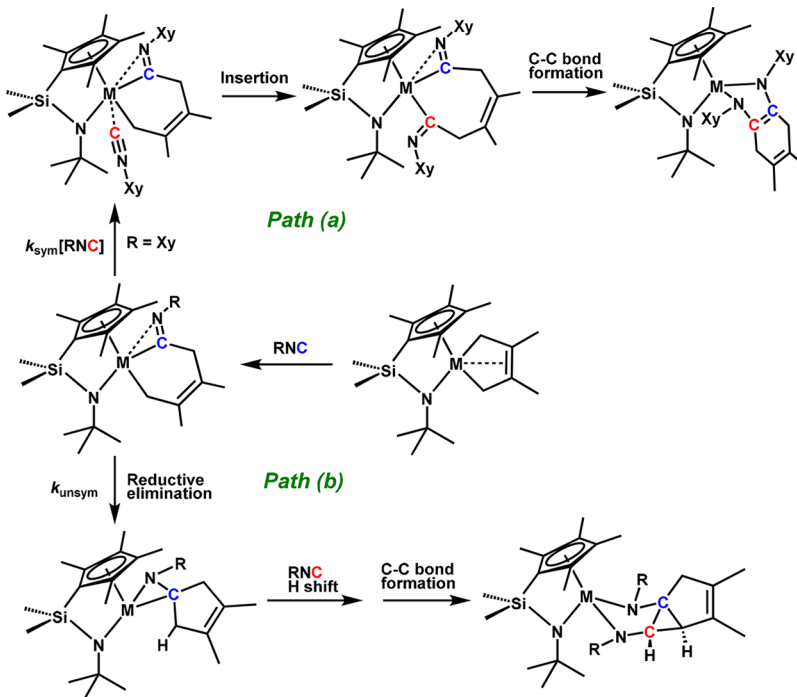
$^1J_{CC}$ for the coordinated cyclopropane increases to 3.5 Hz in 4 (Hf, $^3\text{BuNC}$) and to 6.6 Hz in 6-Hf (XyNC), whereas it is 4.8 Hz in 6-Zr. As mentioned before, the bond length of coordinated C–C in 4 is 1.585(2) Å, considerably longer than the other C–C bonds (1.528(2) and 1.527(2) Å) in the cyclopropane ring.

*Proposed Mechanisms for Isonitrile Insertion into *c*gM-(DMB).* We propose the mechanism in Scheme 4 for the selective formation of the unsymmetrical and symmetrical products. The diene complexes 1 react rapidly with the first equivalent of incoming isonitrile to form mono-insertion intermediates like 2. One of two slower reactions follows: either (a) coordination of a second isonitrile, or (b) reductive elimination and formation of a metalla-aziridine. If (a), the second RNC inserts and the resulting iminoacyl ligands couple, giving a symmetrical bis-insertion product like 5 or 7. If (b), the mono-iminoacyl

By using ^{13}C -enriched isonitriles (eq 9) we have prepared these complexes with their coordinated carbons labeled with ^{13}C , and have been able to determine $^1J_{CC}$ for them (Figure 5). Etienne has demonstrated that this coupling constant (12.4 Hz in free cyclopropane) decreases as the interaction of C–C with the metal becomes stronger.^{32,34} We have already reported^{13a} that $^1J_{CC}$ for a cyclopropane (with xylyl substituents) coordinated to $\text{Cp}^*\text{Hf}(\text{Cl})$ is only 1.1 Hz with an elongated C–C distance of 1.552(9) Å, and have now found that $^1J_{CC}$ only increases slightly (to 1.4 Hz) when the xylyl is replaced with ^3Bu . In the complexes,

Figure 5. $^1J_{CC}$ for the coordinated C–C bonds in our cyclopropane complexes.

Scheme 4. Proposed Mechanisms for the Formation of Two Different Bis-Insertion Isomers



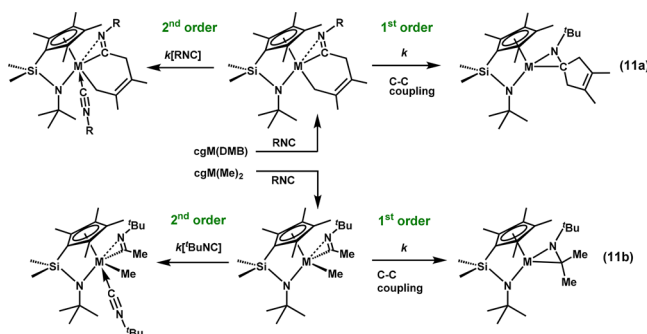
intermediate undergoes reductive elimination to form the metallaziridine, which rearranges to the cyclopropane-containing unsymmetrical bis-insertion product (4 or 6). Of course the rate of (a) depends on $[RNC]$, while the rate of (b) should not. The product distribution should be that in eq 10, in agreement with the results we have observed for eqs 7 and 8 as the order of addition and/or $[RNC]$ is varied.

$$\frac{[\text{sym}]}{[\text{unsym}]} = \frac{k_{\text{sym}}[RNC]}{k_{\text{unsym}}} \quad (10)$$

2. Reaction of Isonitriles with $cgM(Me)_2$ Complexes.

The complexity of the $cgM(\text{diene})/\text{RNC}$ reactions just described has unfortunately made it difficult to look at their mechanisms in detail (Scheme 4 and eq 11a), and reactions 5–8 have all proven too fast to monitor by NMR, even at -60°C . We have therefore looked at the kinetics of RNC insertion into the M–C bonds of simpler constrained geometry systems, $cgM(\text{CH}_3)_2$ ($M = \text{Ti}$ and Hf). In eq 11b the first insertion remains (as it was in eq 11a) too fast to monitor, but the subsequent insertions/rearrangements have proven ideal for NMR rate measurement.

2.1. Structures Arising from Isonitrile Insertion into $cgM-\text{Me}$ Bonds. Ti–Me Bonds. The first insertion of $^t\text{BuNC}$ into a Ti–Me bond of $cg\text{Ti}(\text{Me})_2$ was rapid and gave the mono-iminoacyl



compounds 8-Ti (eq 12 in Figure 6). The ^{13}C NMR ($\delta 240.5$) showed only one signal for the iminoacyl carbon. We anticipated the initial formation of the *outside* isomer 8o-Ti, (1) from the example of 2-Hf in eq 6, and (2) from the location of the vacant orbital available to the incoming lone pair of the isonitrile. (For CO an “outside” stereochemistry was predicted by Lauher and Hoffmann,³⁵ and observed with Cp_2ZrAr_2 by Erker and Rosenfeldt.³⁶) However, SC-XRD analysis (Figure 6) of crystals isolated from reaction eq 12 showed the *inside* isomer 8i-Ti.

The interconversion of “outside” and “inside” iminoacyls only requires rotation about the M–C bond, of the transient η^1 isomer, and is often facile.^{16n,37,38} We see only one set of signals

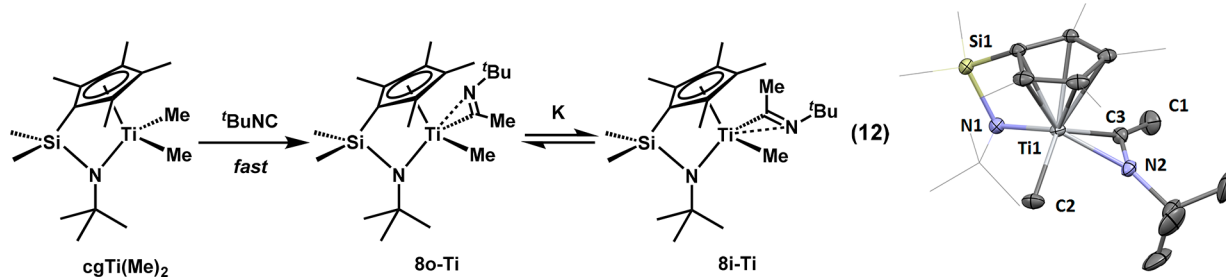


Figure 6. Structure of 8i-Ti . Selected interatomic distances (\AA) and angles (deg): A) Ti1-N1 1.972(2), Ti1-N2 2.073(2), Ti1-C2 2.177(2), Ti1-C3 2.070(2), N2-C3 1.258(3).

from 8-Ti in solution (C_6D_6). The X-ray results suggest that the “inside” isomer of 8-Ti is more stable (as it is in the Zr acyl that Erker and Rosenfeldt examined³⁶). Jordan and Guram also observed the “inside” isomer of $\text{Cp}_2\text{Zr}[\eta^2\text{-CN}('t\text{Bu})\text{Me}](\text{Me})$ in the solid state, and evidence for rapid exchange in a CD_2Cl_2 solution.³⁹

The reaction of 8-Ti with a second equivalent of $^t\text{BuNC}$ (eq 13 in Figure 7) results in 9 , which contains (SC-XRD

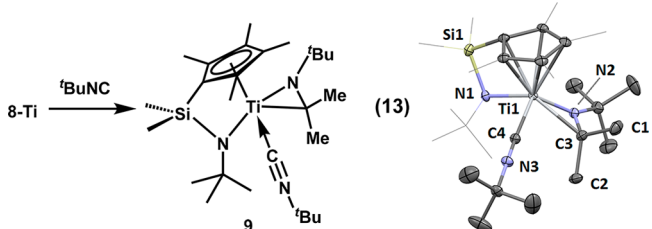
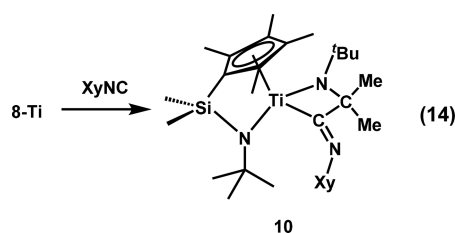


Figure 7. Structure of 9 . Selected interatomic distances (\AA) and angles (deg): A) Ti1-N1 2.011(2), Ti1-N2 1.910(2), Ti1-C3 2.229(2), Ti1-C4 2.154(2), N2-C3 1.402(3), C4-N3 1.158(3).

structure) an isonitrile coordinated to a titana-aziridine. The ^{13}C NMR of 9 shows the coordinated $^t\text{BuNC}$ at δ 174.2; the $\text{C}-\text{N}-\text{C}$ angle of 178.65° reflects (as in the case of 3 above) very little backbonding.^{16g,o,17a,30} The titana-aziridine is presumably the result of methyl/isonitryl coupling—a reaction that has been reported before, albeit without mechanistic investigation.^{16k,m,17e,18,40}

However, replacing the second $^t\text{BuNC}$ in eq 13 with XyNC (eq 14) gave the insertion product 10 (SC-XRD, see Figure 8!).



Apparently XyNC is more reactive than $^t\text{BuNC}$ —a result of which there are previous examples.^{15a,41} The four-membered ring in 10 is distorted by interaction of the Ti with C_β as in $\text{Cp}_2\text{Ti}(\text{CH}_2\text{CMe}_2\text{CH}_2)$.⁴² The $\text{Ti}-\text{C}_\alpha-\text{C}_\beta$ angle is only $86.47(9)^\circ$; the C4-C3 ($\text{C}_\alpha-\text{C}_\beta$) distance, 1.588(2) \AA , is longer than a typical $\text{C}-\text{C}$ bond; the $\text{Ti}\cdots\text{C}_\beta$ distance is only 2.556 \AA . The ^{13}C -labeled 10 , prepared by the reaction of $\text{cgTi}(\text{Me})_2$ with 1 equiv of $^t\text{BuN}^{13}\text{C}$ and then 1 equiv of XyN^{13}C , showed a $^1\text{J}_{\text{CC}}$ (between C4 and C3) of 14.8 Hz, considerably lower than its value in free cyclobutanes (28–29 Hz).⁴²

Hf-Me Bonds. We then investigated the insertion of $^t\text{BuNC}$ into the $\text{Hf}-\text{Me}$ bonds of $\text{cgHf}(\text{Me})_2$. The first insertion is fast, like that of the Ti analogue. However, the second one is relatively slow and easily followed by ^1H NMR; 11 is the only product (eq 15 in Figure 9).

In the SC-XRD structure of 11 (Figure 9), the two iminoacyl groups are placed in a twisted orientation that makes them inequivalent. One iminoacyl adopts an N -outside η^2 orientation, while the other is also η^2 but with its nitrogen pointing away from the Cp ring. However, the ^1H NMR shows only one set of iminoacyl signals, indicative of a mirror plane, and the ^{13}C NMR shows only one iminoacyl carbon (δ 254.4). The rotation of the iminoacyl groups about their metal–carbon bonds must be fast in solution on the NMR time scale.

2.2. Mechanism of Isonitrile Insertion into cgM-Me Bonds. The insertion reactions just described (in Section 2.1) proved slow enough that it was possible to monitor them by ^1H NMR. We examined $\text{cgTi}(\text{Me})_2$ in the presence of an excess of $^t\text{BuNC}$ at 25 $^\circ\text{C}$ in C_6D_6 , then we replaced the $^t\text{BuNC}$ with XyNC , then we looked at $\text{cgHf}(\text{Me})_2$ under the same conditions in the presence of an excess of $^t\text{BuNC}$.

Ti-C Bonds. When $\text{cgTi}(\text{Me})_2$ is treated with an excess of $^t\text{BuNC}$, the first equivalent reacts rapidly to afford 8-Ti . The reaction of 8-Ti with a second equivalent of $^t\text{BuNC}$ (eq 13) forms 9 much more slowly. Its rate is first order in 8-Ti but (Figure 10) zero order in $^t\text{BuNC}$; k_{obs} is $8.2(2) \times 10^{-5} \text{ s}^{-1}$ at 25 $^\circ\text{C}$. No intermediate is observed. The rate-determining step must be the formation of 12 by coupling of the methyl ligand to

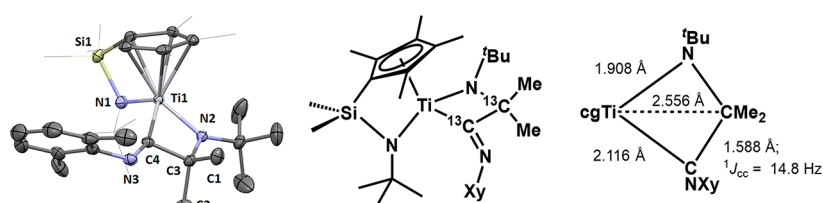


Figure 8. Structure of 10 . Selected interatomic distances (\AA) and angles (deg): Ti1-N1 1.984(1), Ti1-N2 1.908(1), Ti1-C4 2.116(2), $\text{Ti1}\cdots\text{C3}$ 2.556, C3-C4 1.588(2), N2-C3 1.506(2), N3-C4 1.270(2); Ti1-C4-C3 86.47(9).

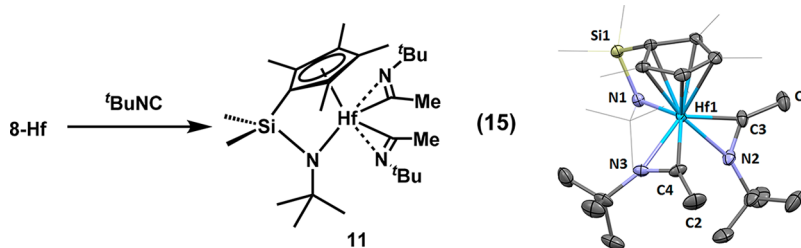


Figure 9. Structure of **11**. Selected interatomic distances (Å) and angles (deg): Hf1–N1 2.166(2), Hf1–N2 2.242(2), Hf1–N3 2.286(2), Hf1–C3 2.206(2), Hf1–C4 2.247(2), N2–C3 1.278(4), N3–C4 1.285(4).

the iminoacyl carbon, with rate constant k_1 ; on geometric grounds it seems reasonable to presume that the outside isomer of **8-Ti** (**8o-Ti**) is the one that reacts. The coupling reaction must be reversible, as **8-Ti** is stable for days (no change by ^1H NMR) in the absence of free isonitrile. The coordination of the second $^t\text{BuNC}$ (rate constant k_2) must be fast. No further reaction is observed for **9**.

The complete mechanism is shown in **eq 16**. In the presence of excess RNC, the steady-state approximation for **12** gives the rate law in **eq 17**. If $k_2[\text{RNC}]$ is much greater than k_{-1} , the rate constant can be reduced to k_1 (**eq 18**), which agrees with the observation that k_{obs} is independent of initial RNC concentration. Correction for the **8o-Ti**/**8i-Ti** equilibrium gives **eq 19**.

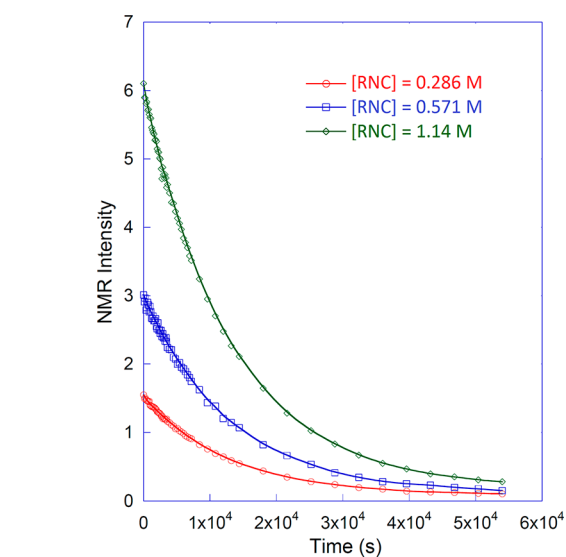
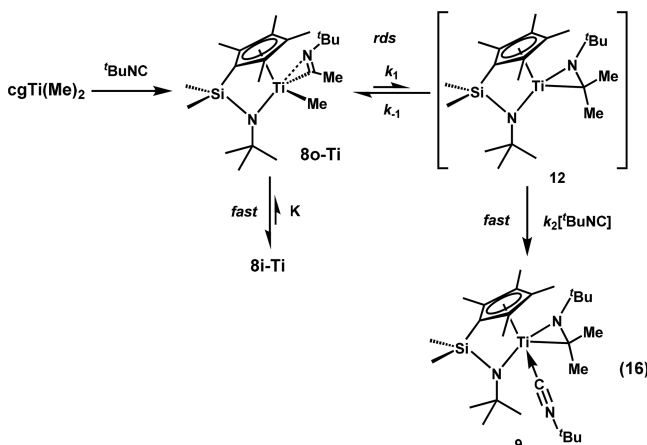
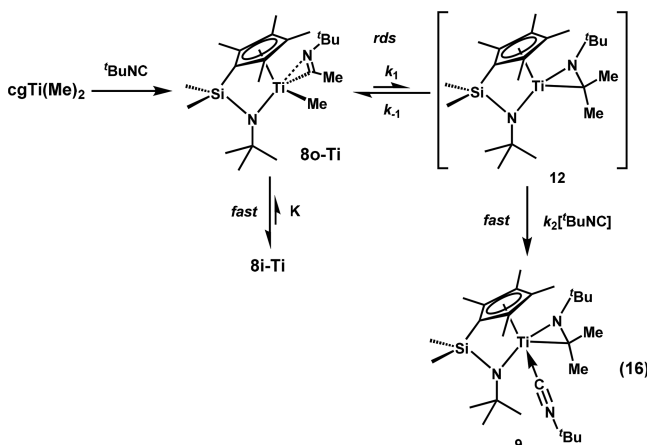


Figure 10. Kinetic studies with different $[^t\text{BuNC}]$ concentrations (red: $k_{\text{obs}} = 8.40 \times 10^{-5} \text{ s}^{-1}$ with $[^t\text{BuNC}] = 0.286 \text{ M}$; blue: $k_{\text{obs}} = 8.06 \times 10^{-5} \text{ s}^{-1}$ with $[^t\text{BuNC}] = 0.571 \text{ M}$; green: $k_{\text{obs}} = 8.17 \times 10^{-5} \text{ s}^{-1}$ with $[^t\text{BuNC}] = 1.14 \text{ M}$). The averaged k_{obs} is $8.2(2) \times 10^{-5} \text{ s}^{-1}$.



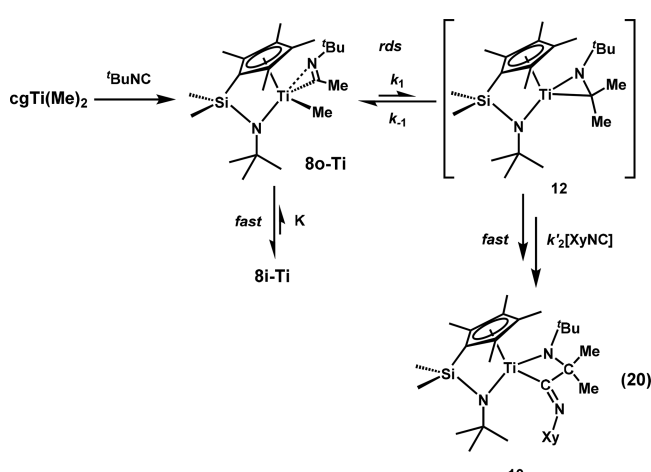
$$\frac{d[9]}{dt} = k_{\text{ss}}[8\text{o-Ti}], \quad \text{where } k_{\text{ss}} = \left(\frac{k_1 k_2 [\text{RNC}]}{k_{-1} + k_2 [\text{RNC}]} \right) \quad (17)$$

$$\text{if } k_{-1} \ll k_2[\text{RNC}], \quad k_{\text{ss}} = k_1 \quad (18)$$

$$\frac{d[9]}{dt} = k_{\text{obs}}[8\text{-Ti}], \quad \text{where } k_{\text{obs}} = k_1 \left(\frac{K}{K + 1} \right) \quad (19)$$

The observation of a rate law zero order in the concentration of RNC implies that the rate should be independent of the *nature* of RNC. Indeed, similar k_{obs} values ($8.68 \times 10^{-5} \text{ s}^{-1}$ and $8.43 \times 10^{-5} \text{ s}^{-1}$ at $[\text{XyNC}] = 0.114$ and 0.571 M , respectively) were observed with XyNC at 25°C . However, instead of yielding a titana-aziridine like **9**, XyNC gave the insertion product titana-azacyclobutane **10** (**eq 20**).

Hf–C Bonds. In our study of the kinetics of the reaction of $\text{cgHf}(\text{Me})_2$ with excess $^t\text{BuNC}$, we only observed the NMR signals of **8-Hf** (the mono-iminoacyl Hf complex) and the bis-insertion product **11**, suggesting that the coordination of the



isonitrile by **8-Hf** is rate-determining. The reaction is pseudo-first-order in the presence of excess $^t\text{BuNC}$, with rate constant k_{obs} . A plot of $k_{\text{obs}}(25^\circ\text{C})$ against the concentration of $^t\text{BuNC}$ is linear (**Figure 11**), with a slope of $1.67(3) \times 10^{-5} \text{ M}^{-1} \text{ s}^{-1}$ —presumably the value of k_3 at that temperature. If we assume that insertion of the coordinated RNC is relatively fast, the mechanism is that given in **eq 21**. The overall rate law is given in **eq 22**.

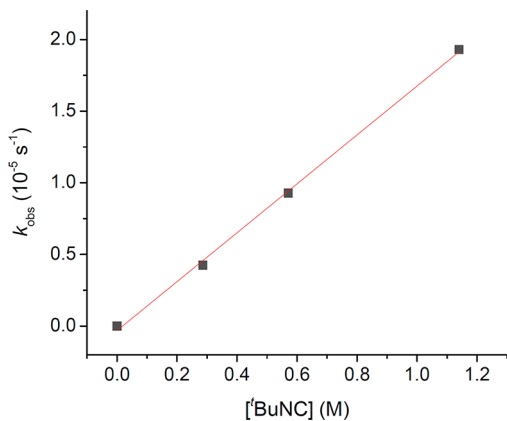
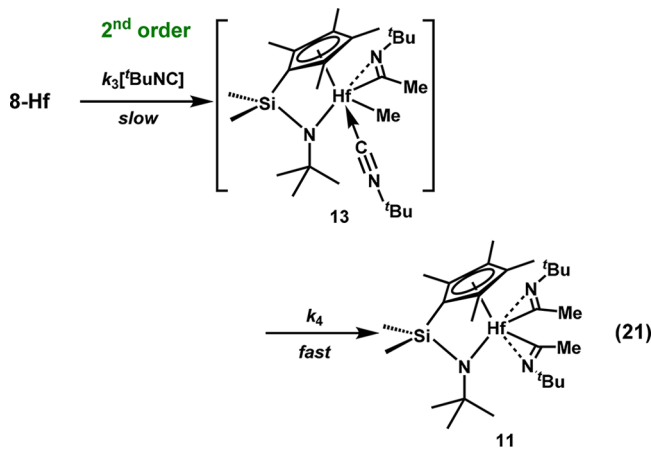


Figure 11. Plot of k_{obs} vs $[\text{BuNC}]$: (a) $k_{\text{obs}} = 4.24 \times 10^{-6} \text{ s}^{-1}$ with $[\text{BuNC}] = 0.286 \text{ M}$; (b) $k_{\text{obs}} = 9.28 \times 10^{-6} \text{ s}^{-1}$ with $[\text{BuNC}] = 0.571 \text{ M}$; (c) $k_{\text{obs}} = 1.93 \times 10^{-5} \text{ s}^{-1}$ with $[\text{BuNC}] = 1.14 \text{ M}$. The linear fit gives $k_3 = 1.67(3) \times 10^{-5} \text{ M}^{-1} \text{ s}^{-1}$.



$$\frac{d[11]}{dt} = k_3[\text{RNC}][8\text{-Hf}] \quad (22)$$

SUMMARY AND CONCLUSIONS

In the case of the 2,3-dimethylbutadiene complex of cgTi , the insertion of one RNC is followed by reductive elimination to form a coordinated cyclopentenimine (the [4+1] cycloaddition product). The 2,3-dimethylbutadiene complexes of Hf and Zr show two competing reactions: (1) the formation of a coordinated cyclopentenimine that can be further converted to an unsymmetrical product with a coordinated cyclopropane (Path (b), **Scheme 4**), and (2) the coordination/embedding of a second RNC to give a symmetrical enediamide product (Path (a), **Scheme 4**). The product ratio will depend upon [RNC].

The reactions of $\text{cg}/(\text{Group 4})$ dimethyl complexes with excess RNC are similar but more suitable for kinetic study. $\text{CgTi}(\text{Me})_2$ complex inserts one RNC rapidly, then does reductive elimination in the rate-determining step (independent of the concentration and nature of RNC, **eqs 16** and **20**). $\text{CgHf}(\text{Me})_2$ coordinates a second RNC (without reductive elimination) to form the symmetrical product; the reaction is first order in RNC.

No intermediates are observed during the insertion of RNC into the Hf–Me bond of **8-Hf**, and the kinetics are first order in RNC—results that are consistent with calculations suggesting that the energy barrier for coordination is higher than that for the insertion itself.¹⁸ However, in some Ti cases coordination of the second isonitrile occurs only *after* C–C coupling; the

resulting isonitrile-coordinated complexes (**3** and **9**) do not undergo insertion.

Alkyl iminoacyl titanium complexes *do not react associatively* with excess isonitrile, but the hafnium/zirconium ones do. The Ti complexes undergo reductive elimination instead. For Hf/Zr that reaction competes with the associative RNC coordination, giving a mixture of the unsymmetrical and symmetrical products.

ASSOCIATED CONTENT

Supporting Information

The Supporting Information is available free of charge on the ACS Publications website at DOI: 10.1021/jacs.8b05377.

X-ray crystallographic data for all prone/supine combinations of **1-Ti**, **1-Zr**, and **1-Hf** (**CIF**)

Full experimental details and additional figures (**PDF**)

AUTHOR INFORMATION

Corresponding Author

* jrn11@columbia.edu

ORCID

Jiawei Chen: 0000-0003-2671-4696

Thilina Gunasekara: 0000-0003-0821-7944

Jack R. Norton: 0000-0003-1563-9555

Notes

The authors declare no competing financial interest.

ACKNOWLEDGMENTS

This work was supported by the National Science Foundation (CHE-1664566). We thank Boulder Scientific Co. for a gift of the cg ligand and Prof. Ged Parkin for access to the SC-XRD instrument. M.R. acknowledges the National Science Foundation for a Graduate Research Fellowship under Grant No. DGE-16-44869.

REFERENCES

- (1) Vogel, P.; Turks, M.; Bouchez, L.; Markovic, D.; Varela-Alvarez, A.; Sordo, J. A. *Acc. Chem. Res.* **2007**, *40*, 931.
- (2) Gibson, S. E.; Stevenazzi, A. *Angew. Chem., Int. Ed.* **2003**, *42*, 1800.
- (3) The transformation proceeds through the addition of a 1,3-dithienium cation to the diene, deprotonation, and hydrolysis: Corey, E. J.; Walinsky, S. W. *J. Am. Chem. Soc.* **1972**, *94*, 8932.
- (4) (a) Franckneumann, M.; Vernier, J. M. *Tetrahedron Lett.* **1992**, *33*, 7365. (b) Franckneumann, M.; Michelotti, E. L.; Simler, R.; Vernier, J. M. *Tetrahedron Lett.* **1992**, *33*, 7361.
- (5) Eaton, B. E.; Rollman, B.; Kaduk, J. A. *J. Am. Chem. Soc.* **1992**, *114*, 6245.
- (6) The carbonylation of 2,3-dimethylbutadiene has been reported in the patent literature, but the conditions are drastic and involve the use of an Ag-lined autoclave: (a) Raasch, M. S.; Theobald, C. W. U.S. Patent US2418850, 1947. Chatani has noted that “no example[s] but stoichiometric” have been reported for this transformation: (b) Tobisu, M.; Chatani, N. *Chem. Lett.* **2011**, *40*, 330.
- (7) *Spartan '10*; Wavefunction, Inc., Irvine, CA, 2010.
- (8) Ito, Y.; Kato, H.; Saegusa, T. *J. Org. Chem.* **1982**, *47*, 741.
- (9) Tobisu, M.; Oshita, M.; Yoshioka, S.; Kitajima, A.; Chatani, N. *Pure Appl. Chem.* **2006**, *78*, 275.
- (10) Tamao, K.; Kobayashi, K.; Ito, Y. *J. Am. Chem. Soc.* **1988**, *110*, 1286.
- (11) Berk, S. C.; Grossman, R. B.; Buchwald, S. L. *J. Am. Chem. Soc.* **1994**, *116*, 8593.
- (12) (a) Nakamura, A.; Mashima, K. *J. Organomet. Chem.* **2004**, *689*, 4552. (b) Erker, G.; Kruger, C.; Muller, G. *Adv. Organomet. Chem.* **1985**, *24*, 1.

(13) (a) Valadez, T. N.; Norton, J. R.; Neary, M. C. *J. Am. Chem. Soc.* **2015**, *137*, 10152. (b) Valadez, T. N.; Norton, J. R.; Neary, M. C.; Quinlivan, P. J. *Organometallics* **2016**, *35*, 3163.

(14) The mechanisms of these reactions have been examined by computational methods in the recent papers of Zhang and Wang: (a) Du, M. R.; Zhang, X. B.; Yang, F.; Hou, C. M. *Comput. Theor. Chem.* **2017**, *1117*, 177. (b) Du, M. R.; Zhang, X. B.; Si, S. M.; Yang, F.; Wang, L. *RSC Adv.* **2017**, *7*, 34816. (c) Du, M. R.; Zhang, X. B.; Si, S. M.; Wang, L. *RSC Adv.* **2017**, *7*, 44979.

(15) For reviews on the insertion of isonitriles into metal–element bonds, see: (a) Boyarskiy, V. P.; Bokach, N. A.; Luzyanin, K. V.; Kukushkin, V. Y. *Chem. Rev.* **2015**, *115*, 2698. (b) Lauzon, J. M. P.; Schafer, L. L. *Dalton Trans.* **2012**, *41*, 11539. (c) Durfee, L. D.; Rothwell, I. P. *Chem. Rev.* **1988**, *88*, 1059.

(16) For selected examples of isonitrile insertion into Group 4 M–C bonds, see: (a) Batke, S.; Sietzen, M.; Merz, L.; Wadeppohl, H.; Ballmann, J. *Organometallics* **2016**, *35*, 2294. (b) Fernandez-Galan, R.; Antinolo, A.; Carrillo-Hermosilla, F.; Lopez-Solera, I.; Otero, A.; Serrano-Laguna, A.; Villasenor, E. *Organometallics* **2012**, *31*, 8360. (c) Waterman, R.; Tilley, T. D. *Chem. Sci.* **2011**, *2*, 1320. (d) Thomson, R. K.; Schafer, L. L. *Organometallics* **2010**, *29*, 3546. (e) Spencer, L. P.; Fryzuk, M. D. *J. Organomet. Chem.* **2005**, *690*, 5788. (f) Ong, T. G.; Wood, D.; Yap, G. P. A.; Richeson, D. S. *Organometallics* **2002**, *21*, 1. (g) Santamaria, C.; Beckhaus, R.; Haase, D.; Koch, R.; Saak, W.; Strauss, I. *Organometallics* **2001**, *20*, 1354. (h) Antinolo, A.; Carrillo-Hermosilla, F.; Corrochano, A.; Fernandez-Baeza, J.; Lara-Sanchez, A.; Ribeiro, M. R.; Lanfranchi, M.; Otero, A.; Pellinghelli, M. A.; Portela, M. F.; Santos, J. V. *Organometallics* **2000**, *19*, 2837. (i) Andres, R.; Galakhov, M.; Gomez-Sal, M. P.; Martin, A.; Mena, M.; Santamaria, C. *Chem. - Eur. J.* **1998**, *4*, 1206. (j) Ahlers, W.; Erker, G.; Frohlich, R. *J. Organomet. Chem.* **1998**, *571*, 83. (k) Scott, M. J.; Lippard, S. J. *Organometallics* **1997**, *16*, 5857. (l) Kloppenburg, L.; Petersen, J. L. *Organometallics* **1997**, *16*, 3548. (m) Giannini, L.; Caselli, A.; Solari, E.; Floriani, C.; ChiesiVilla, A.; Rizzoli, C.; Re, N.; Sgamellotti, A. *J. Am. Chem. Soc.* **1997**, *119*, 9709. (n) Chamberlain, L. R.; Durfee, L. D.; Fanwick, P. E.; Kobriger, L.; Latesky, S. L.; McMullen, A. K.; Rothwell, I. P.; Folting, K.; Huffman, J. C.; Streib, W. E.; Wang, R. *J. Am. Chem. Soc.* **1987**, *109*, 390. (o) Bochmann, M.; Wilson, L. M.; Hursthouse, M. B.; Short, R. L. *Organometallics* **1987**, *6*, 2556. (p) Beshouri, S. M.; Fanwick, P. E.; Rothwell, I. P.; Huffman, J. C. *Organometallics* **1987**, *6*, 891.

(17) For selected examples of isonitrile insertion into Group 4 metallacycles, see: (a) Bach, M. A.; Beweries, T.; Burlakov, V. V.; Arndt, P.; Baumann, W.; Spannenberg, A.; Rosenthal, U. *Organometallics* **2007**, *26*, 4592. (b) Ramakrishna, T. V. V.; Lushnikova, S.; Sharp, P. R. *Organometallics* **2002**, *21*, 5685. (c) Greidanus-Strom, G.; Carter, C. A. G.; Stryker, J. M. *Organometallics* **2002**, *21*, 1011. (d) Takahashi, T.; Tsai, F. Y.; Li, Y. Z.; Nakajima, K. *Organometallics* **2001**, *20*, 4122. (e) Thorn, M. G.; Fanwick, P. E.; Rothwell, I. P. *Organometallics* **1999**, *18*, 4442. (f) Cadiero, V.; Zablocka, M.; Donnadieu, B.; Igau, A.; Majoral, J. P.; Skowronska, A. *J. Am. Chem. Soc.* **1999**, *121*, 11086. (g) Campora, J.; Buchwald, S. L.; Gutierrezpuebla, E.; Monge, A. *Organometallics* **1995**, *14*, 2039. (h) Hill, J. E.; Balaich, G.; Fanwick, P. E.; Rothwell, I. P. *Organometallics* **1993**, *12*, 2911. (i) Berg, F. J.; Petersen, J. L. *Organometallics* **1993**, *12*, 3890. (j) Berg, F. J.; Petersen, J. L. *Organometallics* **1991**, *10*, 1599. (k) Berg, F. J.; Petersen, J. L. *Organometallics* **1989**, *8*, 2461.

(18) De Angelis, F.; Fantacci, S.; Sgamellotti, A.; Re, N. *Theor. Chem. Acc.* **2003**, *110*, 196.

(19) (a) Shapiro, P. J.; Cotter, W. D.; Schaefer, W. P.; Labinger, J. A.; Bercaw, J. E. *J. Am. Chem. Soc.* **1994**, *116*, 4623. (b) Shapiro, P. J.; Bunel, E.; Schaefer, W. P.; Bercaw, J. E. *Organometallics* **1990**, *9*, 867.

(20) (a) Cano, J.; Kunz, K. *J. Organomet. Chem.* **2007**, *692*, 4411. (b) Braunschweig, H.; Breitling, F. M. *Coord. Chem. Rev.* **2006**, *250*, 2691.

(21) (a) Gibson, V. C.; Spitzmesser, S. K. *Chem. Rev.* **2003**, *103*, 283. (b) Chum, P. S.; Kruper, W. J.; Guest, M. J. *Adv. Mater.* **2000**, *12*, 1759. (c) McKnight, A. L.; Waymouth, R. M. *Chem. Rev.* **1998**, *98*, 2587.

(d) Brintzinger, H. H.; Fischer, D.; Mülhaupt, R.; Rieger, B.; Waymouth, R. M. *Angew. Chem., Int. Ed. Engl.* **1995**, *34*, 1143.

(22) Kristian, K. E.; Iimura, M.; Cummings, S. A.; Norton, J. R.; Janak, K. E.; Pang, K. *Organometallics* **2009**, *28*, 493.

(23) (a) Devore, D. D.; Timmers, F. J.; Hasha, D. L.; Rosen, R. K.; Marks, T. J.; Deck, P. A.; Stern, C. L. *Organometallics* **1995**, *14*, 3132. (b) Devore, D. D.; Timmers, F. J.; Stevens, J. C.; Rosen, R. K. *Int. Patent* WO9600734A1, 1996.

(24) Dahlmann, M.; Schottek, J.; Frohlich, R.; Kunz, D.; Nissinen, M.; Erker, G.; Fink, G.; Kleinschmidt, R. *J. Chem. Soc., Dalton Trans.* **2000**, 1881.

(25) (a) Strauch, J. W.; Petersen, J. L. *Organometallics* **2001**, *20*, 2623. (b) Braun, L. F.; Dreier, T.; Christy, M.; Petersen, J. L. *Inorg. Chem.* **2004**, *43*, 3976.

(26) (a) Chen, Y. X.; Marks, T. J. *Organometallics* **1997**, *16*, 3649. (b) Devore, D. D.; Neithamer, D. R.; Lapointe, R. E.; Mussell, R. D. *Int. Patent* WO9608519A2, 1996.

(27) A “supine” diene has its open end toward the Cp ring, and a “prone” diene has its open end away from the Cp ring: Yasuda, H.; Tatsumi, K.; Okamoto, T.; Mashima, K.; Lee, K.; Nakamura, A.; Kai, Y.; Kanehisa, N.; Kasai, N. *J. Am. Chem. Soc.* **1985**, *107*, 2410.

(28) The differences in length between the terminal C–C and internal C–C bonds (ΔCC) and terminal and internal metal–carbon bonds (ΔMC) have been used to gauge the most accurate description of the bonding in cg diene complexes. In typical cgTi(diene) complexes with the prone orientation and π^2 bonding, such as cgTi(2,4-hexadiene), $\Delta CC = -0.007 \text{ \AA}$ and $\Delta MC = 0.011 \text{ \AA}$; in cgTi(1,3-butadiene), $\Delta CC = -0.039 \text{ \AA}$ and $\Delta MC = 0.080 \text{ \AA}$.

(29) For cgZr(butadiene) reported by Erker and co-workers in ref 24, $\Delta MC = 0.159 \text{ \AA}$ and $\Delta CC = 0.077 \text{ \AA}$.

(30) For examples of isonitrile coordination to d⁰ Group 4 metals, see: (a) Altenburger, K.; Arndt, P.; Becker, L.; Reiss, F.; Burlakov, V. V.; Spannenberg, A.; Baumann, W.; Rosenthal, U. *Chem. - Eur. J.* **2016**, *22*, 9169. (b) Podiyanchari, S. K.; Kehr, G.; Muck-Lichtenfeld, C.; Daniliuc, C. G.; Erker, G. *J. Am. Chem. Soc.* **2013**, *135*, 17444. (c) Suzuki, N.; Hashizume, D.; Yoshida, H.; Tezuka, M.; Ida, K.; Nagashima, S.; Chihara, T. *J. Am. Chem. Soc.* **2009**, *131*, 2050. (d) Tamm, M.; Kunst, A.; Bannenberg, T.; Herdtweck, E.; Schmid, R. *Organometallics* **2005**, *24*, 3163. (e) Hair, G. S.; Jones, R. A.; Cowley, A. H.; Lynch, V. *Organometallics* **2001**, *20*, 177. (f) Strauch, H. C.; Wibbeling, B.; Frohlich, R.; Erker, G.; Jacobsen, H.; Berke, H. *Organometallics* **1999**, *18*, 3802. (g) Brackemeyer, T.; Erker, G.; Frohlich, R. *Organometallics* **1997**, *16*, 531.

(31) For definition of “inside” and “outside” isomers, see: Tatsumi, K.; Nakamura, A.; Hofmann, P.; Stauffert, P.; Hoffmann, R. *J. Am. Chem. Soc.* **1985**, *107*, 4440.

(32) Etienne, M.; Weller, A. S. *Chem. Soc. Rev.* **2014**, *43*, 242.

(33) Van Koten, G.; Vrieze, K. *Adv. Organomet. Chem.* **1982**, *21*, 151.

(34) Boulho, C.; Keys, T.; Coppel, Y.; Vendier, L.; Etienne, M.; Locati, A.; Bessac, F.; Maseras, F.; Pantazis, D. A.; McGrady, J. E. *Organometallics* **2009**, *28*, 940.

(35) Lauher, J. W.; Hoffmann, R. *J. Am. Chem. Soc.* **1976**, *98*, 1729.

(36) Erker, G.; Rosenfeldt, F. *Angew. Chem., Int. Ed. Engl.* **1978**, *17*, 605.

(37) (a) Thorn, M. G.; Lee, J.; Fanwick, P. E.; Rothwell, I. P. *J. Am. Chem. Soc., Dalton Trans.* **2002**, 3398. (b) Chen, L. Y.; Nie, W. L.; Paradies, J.; Kehr, G.; Frohlich, R.; Wedeking, K.; Erker, G. *Organometallics* **2006**, *25*, 5333.

(38) In the cgHf(iminoacyl)₂ we synthesized (see below), we observed two inequivalent iminoacyl groups in the X-ray structure, but ¹H NMR shows that their signals average in solution—indicating rapid rotation of the iminoacyl groups.

(39) Guram, A. S.; Jordan, R. F. *J. Org. Chem.* **1993**, *58*, 5595.

(40) Fantacci, S.; De Angelis, F.; Sgamellotti, A.; Re, N. *Organometallics* **2002**, *21*, 4090.

(41) Cano, J.; Sudupe, M.; Royo, P.; Mosquera, M. E. G. *Organometallics* **2005**, *24*, 2424.

(42) These data are consistent with the presence of a C–C σ interaction to Ti, analogous to the σ interaction in titanacyclobutane Cp₂Ti(CH₂CMe₂CH₂) (coordinated C–C bond: 1.583 Å; ¹J_{CC} = 22.0 Hz): Harvey, B. G.; Mayne, C. L.; Arif, A. M.; Ernst, R. D. *J. Am. Chem. Soc.* **2005**, *127*, 16426.